CHAPTER-3

Experimental Methods

3.1 Material

Few researchers have worked on the formation of the OSL rot curve of quartz materials, especially the synthetic quartz case. Vary luminescence complex is shown and shows a variety of objects with different body properties. This complexity is associated with various defects in quartz that may be internal (e.g., Si and O spaces) or related to atoms of contaminants (e.g., Al or Ti). It has been observed by many researchers that the shape of the OSL Decay curve from quartz depends on the physical treatment and the parameters associated with it. For this purpose, in the present study of the manufacture of quartz were selected and given various treatments before studying OSL. The current work protocol (Physical Therapy and Testing Process) has suggested a significant curve for OSL decay from Quartz synthetic. In line with this study, a study of the interaction between OSL and TL of synthetic quartz was performed. In the present work an advanced quartz-made laboratory was selected to study OSL and TL study under a variety of physical conditions for dosimetry and cooling applications.

The laboratory grew synthetic quartz was provided by the Centre of Glass and Ceramic Research Institute (CGCRI), Kolkata. This crystal was prepared using a hydrothermal process of single quartz crystals at high pressure autoclaves at high temperatures. In this chapter, sample preparation and the general definitions of the metals used and the various test methods used are discussed in detail.

3.2 Instruments Used

1. Agate mortar and pestle
2. Weighing balance (AX120, Shimadzu, Japan)
3. Muffle Furnace (up to 1200^0C)
4. TL/OSL Reader (DA20, DTU Nutech, Denmark)
5. ESR

3.3 Sample Preparation

This type of lab-based quartz was crushed using agate mortar and pestle and prepared a fine powder with a grain size of 63-53 μm used for TL / OSL research in the current investigation.

3.4 Thermal Annealing Treatment

The furnace was used to provide the hot heating of the statue made in the furnace. The laboratory furnace has a temperature of up to 1200°C and the sample room temperature was 22cm x 10cm x 10cm. Temperatures were maintained at an accuracy of ± 1 ° C using a temperature controller, which provided much-needed power in the furnace. A 230V power supply was supplied to the furnace. Quartz samples in the form of fine flour with grain size 63-53 μm are stored in four different silica materials in the furnace at different temperatures annealing 400°C, 600°C, 800°C, 1000°C the required time and are quickly dissolved in air at room temperature by retrieving silica crucible in a ceramic block. Such samples or building materials are called "reduced and finished" or "pre-heated treatment template"

3.5 Thermoluminescence analysis

The condition of the thermoluminescence is described in section 1.5.1 TL curve of prepared (unannealed and annealed) synthetic quartz sampled followed by different beta doses were recorded from 0 to 450 ° C with 5 ° Cs^{-1} constant heating rate using Risø TL / OSL (model TL / OSL-DA-20). TL size is typical for the weight of each sample.

3.6 Analysis of Optically Stimulated Luminescence

The condition of the well-promoted Luminescence is well described in paragraph 1.5.2 The state of illuminated renewable light is directly related to electron traps in semiconductors or insulators that occur due to the presence of point defects in the crystal structure. In the case of OSL, radiation is used to transfer carriers into trap levels. This concentration of electrons trapped directly in line with the power of the OSL. Therefore, the relationship between the amount of radiation absorbed by phosphorus and the strength of OSL is widely used in dosimetry[1-2]. In the present study, Continuous Wave OSL (CWOSL) is used for OSL measurement. According to the CWOSL standard, a simple rotation curve is observed when light stimulation is performed with light of continuous length and continuous intensity. OSL rot curve of prepared quartz samples (open and frozen) recorded 0 to 100 seconds at a temperature of 160 0C using a Risø TL / OSL reader (line TL / OSL-DA-20) with a line or -broadband 470 nm to update length. OSL quantity is typical for the weight of each

sample. OSL rot curve is defined by objects. The ORIGIN8.0 software is used to resolve OSL components using the optimal curve decay method.

3.7 Analysis of Electron Spin Resonance

ESR is one of the branches of absorption spectroscopy where radiation has a frequency in the microwave region (0.04-25cm). In this process, radiation is absorbed by the paramagnetic material to induce a change in the magnetic field of the electron with unbroken spins. This absorption of microwave radiation occurs under the influence of the applied magnetic field. Paramagnetic objects have one or more uncharged electrons and therefore, reflect ESR. ESR is also known as electron paramagnetic resonance (EPR).[3] The difference between lower and upper state $\Delta E = g_e \mu_B B_0$is used to calculate g-factor for unpaired free electron. Where, $ge$is Lande g-factor of electrons and μB is Bohr magneton.

The g-factor give the information about electronic structure of a paramagnetic center. Above equation shows that split of energy levels (ΔE) is directly proportional to external magnetic field with (B_0) strength.[3] (Fig. 3.1)

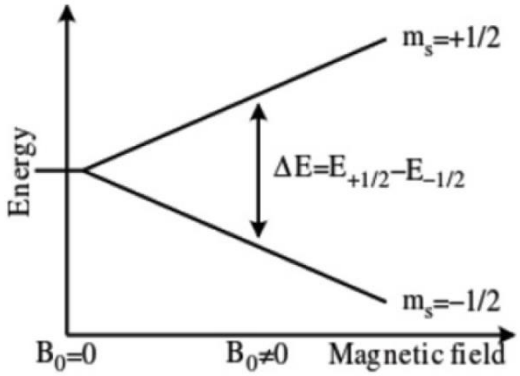

Fig. 3.1 Energy levels of unpaired free electron with respect to applied magneticfield[3].

In present study, ESR signal was used to detect the defect center present in the material which helped to confirm and explain the changes observed in TL and OSL behavior of the synthetic quartz under different physical conditions.

3.8 TL/OSL Reader (DA-20, DTU Nutech, Denmark)

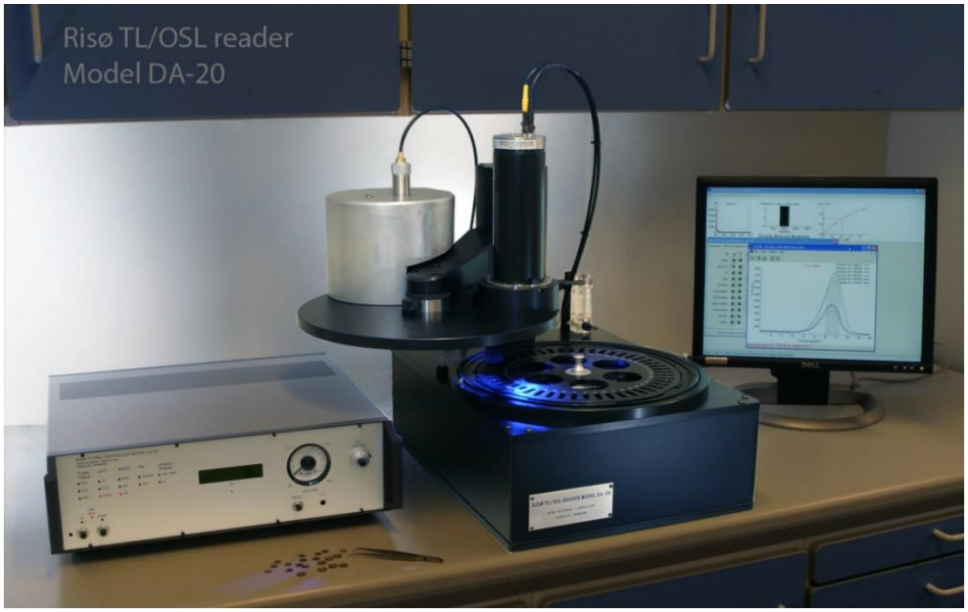

Fig 3.2 The Risø TL/OSL reader (DA-20)[4]

The Risø TL/OSL reader enables automated measurements of thermoluminescence (TL) and Optically Stimulated Luminescence (OSL) signals. As the measurement system is highly sensitive and includes a reference radiation source, it is widely used for determining radiation doses in natural and artificial materials with applications in geological and archaeological dating, forensic and accident dosimetry, and radiation protection. Several state-of-the-art attachments to the TL/OSL reader allow investigations on luminescence physics in different phosphors/dosimeters.

3.8.1 The Risø TL/OSL Reader Model DA-20 consists of:

- Automated 48-position sample changer system built into a vacuum chamber (lowest pressure < 2 x 10^{-2} mbar).
- Two exchangeable sample holders (each designed to hold 48 samples) for 9.7 mm diam. Flat sample discs or 11.65 mm diam. sample cups.
- Vacuum sensing system with automated switching on reaching desired pressure, vacuum gauge, and combined vacuum/nitrogen solenoid valves (exclusive vacuum pump).
- Lift mechanism for heater element.
- Shaped Kanthal heater strip, endpoint temperature: 700^0C.

- Filter holder to allow fitting of different optical detection filters.
- Photomultiplier housing with dynode chain and μ-metal shielding.
- 100 11.65 mm diameter stainless steel sample cups and 100 9.7 mm diameter flat stainless-steel discs

3.8.2 Electronics, detectors and controls

The Risø TL/OSL Controller allows for flexible control of the TL/OSL system including input/output ports, counters, and heat profile generator.

- Continuous full sine wave programmable heating system that can perform a linear heating profile for TL, preheat, and isothermal functions (endpoint: 700^0C).
- Automated software-based function control for activating beta irradiator, atmosphere valves and all mechanical movements.
- Single photon counting amplifier / discriminator system.
- Stabilised, adjustable high-voltage supply for PM tube (max. 1500 V).
- Linear, up to 40 x106 counts per second and low dark count EMI 9235QB15 PM tube.

Fig 3.3 The Risø TL/OSL Controller

3.8.3 Irradiation sources

a) Irradiation

In the Risø TL/OSL reader sample irradiation can be obtained using three different irradiation sources:

i) beta

ii) alpha and

iii) X-ray.

Irradiations are software controlled allowing in-situ irradiations (minimum irradiation time of 1 s).

b) 90Sr/90Y beta source

A detachable beta irradiator is located above the sample carousel providing software-controlled in-situ irradiations of samples. The irradiator normally accommodates a 1.48 GBq (40 mCi) 90Sr/90Y beta source. The dose rate in quartz at the sample position is approximately 0.1 Gy/s. (Sr90-sources with other activities are available on request) The Sr90-source is mounted into a rotating, stainless steel wheel, which is pneumatically controlled. The distance between the source and the sample is 7.6 mm. A 0.125 mm beryllium window is located between the irradiator and the measurement chamber and acts as a vacuum sealing.

c) Beta irradiation system

A detachable beta irradiator is located above the sample carousel and a schematic drawing of the irradiator unit is shown in Figure 3.4. The irradiator is made of brass (outer diameter 10 cm) and is surrounded by 20 mm of lead on the sides, and 40 mm on the top. Furthermore, an aluminum safety helmet (outer diameter 222 mm) covers the entire irradiator and lead shielding.

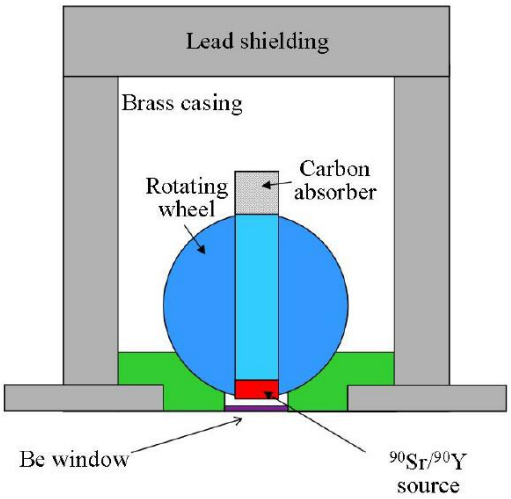

Figure 3.4: Schematic diagram of the cross section of the beta irradiator.

This irradiator accommodates a 90Sr/90Y beta source, which emits beta particles with a maximum energy of 2.27 MeV. The half-life is 30 years. The source strength is usually about 1.48 GBq, which gives a dose rate in quartz at the sample position of approximately 0.1 Gy/s. The source is mounted into a rotating, stainless steel wheel, which is pneumatically activated; it takes the source 0.11 s to rotate from the closed position to the open position (Markey et al., 1997). This offset time is constant for all

irradiations and is negligible for long radiations. In brief irradiations, it can be compensated for by subtracting it from the programmed irradiation time.

The source-to-sample distance should be as small as possible to provide the highest possible dose rate at the sample, however, any spatial variations in dose rate across the source will be accentuated at small source-to-sample distances, so a compromise is required. The distance between the source and the sample is 7 mm. The source is placed inside the irradiator, directly followed by a 20 mm thick aluminum spacer, a 20 mm thick lead spacer, a spring washer, and finally a 25 mm thick aluminum spacer. When the source is “off" (default position) it is pointing upwards directly at a 10 mm Carbon absorber. When the source is “on" (activated position) it is pointing downwards towards the measurement chamber. A 0.125 mm beryllium window is located between the irradiator and the measurement chamber to act as a vacuum interface for the measurement chamber. On a 48 samples carousel, the distance between the centers of adjacent sample positions is 17 mm. The consequence of this close spacing is that irradiation of one sample will lead to a dose being absorbed in the adjacent samples. This phenomenon is referred to as irradiation cross-talk. Thomsen et al. (2006) measured the irradiation cross-talk to be 0.250% ±0.003% for adjacent samples and 0.014%±0.002% for second nearest samples.

d) Beta Irradiator attachment

The irradiator normally accommodates a 1.48 GBq (40 mCi) 90Sr/90Y beta source, which emits beta particles with a maximum energy of 2.27 MeV. The dose rate in quartz at the sample position is approximately 0.1 Gy/s. The detachable on-plate automated beta irradiator including beryllium foil vacuum interface provides software-controlled in-situ irradiations of samples.

Figure 3.5 Beta Irradiator attachment

3.8.4 Infrared/Blue Light Optically Stimulated Luminescence (OSL) attachment

Optical stimulation is achieved using an array of light emitting diodes (LEDs), which are compact, fast and enables electronic control of the illumination power density. The standard system incorporates CW as well as LM-OSL stimulation. The array of LEDs is equipped with an optical feedback servosystem to ensure the stability of the stimulation power. The key component for this process is the combined Infrared/Blue Light stimulated luminescence (IRSL/OSL) unit attachable to the Risø TL sample changer for IRSL/OSL measurements of a variety of natural and artificial materials.

Figure 3.6 Infrared/Blue Light Optically Stimulated Luminescence (OSL) attachment

The OSL unit is based on illumination with

1. clusters of 870 nm IR LEDs providing > 135 mW/cm2 at the sample and
2. clusters of 470 nm blue LEDs delivering > 80 mW/cm2 at sample.

The OSL unit enables flexible and combined BLSL/IRSL/TL measurements in automated sequences. The OSL/IRSL system includes a software-controlled power supply to allow illumination power to be varied during a measurement sequence (e.g.,

for normalization) or to the ramp of the illumination power during an OSL readout to perform linearly modulated OSL (LM-OSL) to investigate trap distributions and OSL decay rate components.

3.8.5 Software

i) Sequence Editor

The Sequence Editor is a flexible MS Windows software that permits the easy creation of any desired automated TL/OSL measurement sequence. These sequences can include any or all operations (e.g., preheat, irradiation, OSL, etc.) individually, or in combination.

The software allows for a large number of operations to be controlled in one measurement sequence. The user may also program the reader operations using a Macro language. Sequences can be stored and recalled for future measurement routines. Live display of TL and OSL signals on the computer screen during a sequencing run is provided. Data is stored in a format accessible by Viewer and Analyst (also provided).

(ii) Control program

The Control program allows the individual units of the reader to be tested. It is mainly used for test, adjustment, and maintenance purposes.

(iii) Viewer

The Viewer is used to display and print curves, perform integration, and export data from the data files.

(iv) Analyst

The analyst is a program designed to view, edit and analyze luminescence data collected using the Risø TL/OSL reader. It allows data to be exported in a variety of formats so that it can be transferred to other programs. An analyst is especially developed for the Risø TL/OSL system by Prof. G.A.T. Duller, University College of Wales, Aberystwyth, UK.

3.8.6 Sample carousel

The sample carousel rests on a motor driven turntable, which enables rotation of the sample carousel. Rotation is computer controlled and position holes drilled though the

carousel in close proximity to the sample positions enable the system to keep track of the position of the carousel using optoelectronics.

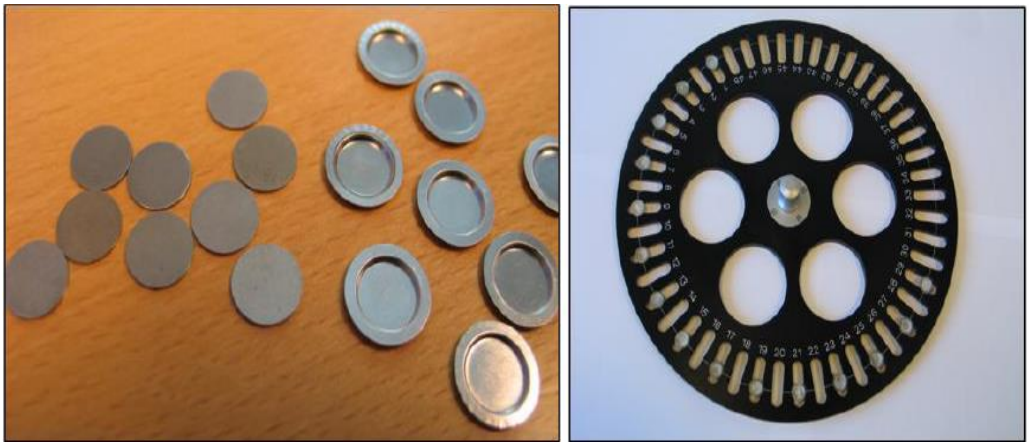

Figure 3.7 Sample discs/cups and sample carrousel

An infrared light emitting diode (LED) is positioned underneath the turntable, which is switched on during rotation. The measurement is initiated by moving a given sample to the measurement position located directly underneath the light detection system. The sample carrousel rotates at two different speeds (two-speed turntable) to reduce processing time. If a sample is moved to the next position then the turntable turns at the normal speed.

3.8.7 Light detection system

The essential components of the light detection system are

1) a photomultiplier tube (PMT) and

2) suitable detection filters.

The detection filters serve both to shield the PMT from scattered stimulation light and to define the spectral detection window.

3.8.8 Photomultiplier tube

The emitted luminescence is detected by a photomultiplier tube (PMT). The light-sensitive component in the PMT is the cathode. This is coated with a photo-emissive substance; CsSb and other bi-alkali compounds are commonly used for this material. Typically, ten photons in the visible range striking the cathode are converted into one

to three electrons. Electrons emitted from the photocathode are accelerated towards a series of dynodes maintained at a positive voltage relative to the photocathode. Electrons with sufficient velocity striking the dynode will eject several secondary electrons from the surface.

The standard PMT in the Riso TL/OSL reader is a bi-alkali EMI 9235QB PMT, which has maximum detection efficiency between 200 and 400 nm, making it suitable for the detection of luminescence from both quartz and feldspar. The PMT is operated in “photon counting" mode, where each pulse of the charge arising at the anode is counted. Many samples are only weakly luminescent making optimization of light collection important. Thus, the PMT must extend as large a solid angle as possible. As the stimulation sources have to be placed between the sample and the PMT the sample-to-PMT cathode distance in the Riso TL/OSL reader is ~ 55 mm, giving a detection solid angle of approximately 0.4 steradians.

3.8.9 Detection filters

The intensity of the stimulation light is approximately $\sim 10^{18}$ orders of magnitude larger than the emitted luminescence. In order to be able to measure the emitted luminescence, detection filters must be used to prevent scattered stimulation light from reaching the PMT, and the spectral stimulation and detection windows must be well separated.

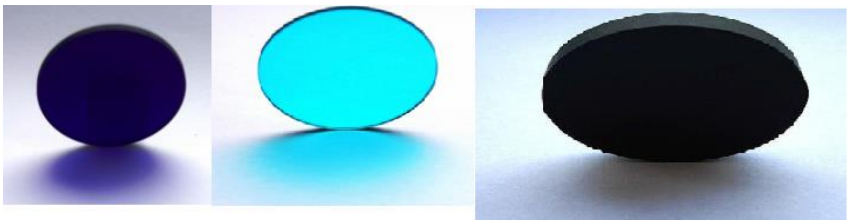

Figure 3.8 Detection Filters

The TL/OSL reader is per default supplied with a set of the following stimulation and detection filters cut to fit the filter holders:

a) 7.5 mm Hoya U-340 b) 2 mm Schott BG-39 c) 3 mm Schott BG-3

Quartz has a strong emission centered on 365 nm (near UV) and many types of feldspars have a strong emission centered on 410 nm (violet). Quartz OSL is often detected using the Hoya U-3402 filter, whereas feldspar OSL often is detected using

the so-called blue filter pack comprising of Schott BG-39 in combination with Corning 7-59 or BG3.

3.8.10 Luminescence stimulation system

The Riso TL/OSL reader has two luminescence stimulation systems: 1) a heating system that can be used for TL measurements and 2) a light stimulation system that can be used for OSL measurements. The two stimulations can be used in combination, e.g. OSL at elevated temperature is possible.

a) Heating system

The heating element and lift mechanism is located directly underneath the photomultiplier tube. The heating element (see Figure 3.9) has two functions: 1) it heats the sample and 2) it lifts the sample into the measurement position.

The heater strip is made of low-mass Kanthal (a high resistance alloy) which is shaped with a depression to provide good heat transmission to the sample and to lift it securely and reproducibly into the measurement position. Heating is accomplished by feeding a controlled current through the heating element. Feedback control of the temperature employs a Cromel-Alumel thermocouple (0.5 mm) mounted underneath the heater strip. The thermocouple is fixed to the heater element using a gold rivet. Heating is provided by a continuous non-switching fixed frequency sine wave generator. The heating system is able to heat samples to 700^0C at constant heating rates from 0.1 to 10 K/s. To minimize thermal lag between sample and heater strip heating rates above 5 K/s are usually not employed. The heating strip can be cooled by a nitrogen ow, which also protects the heating system from oxidation at high temperatures.

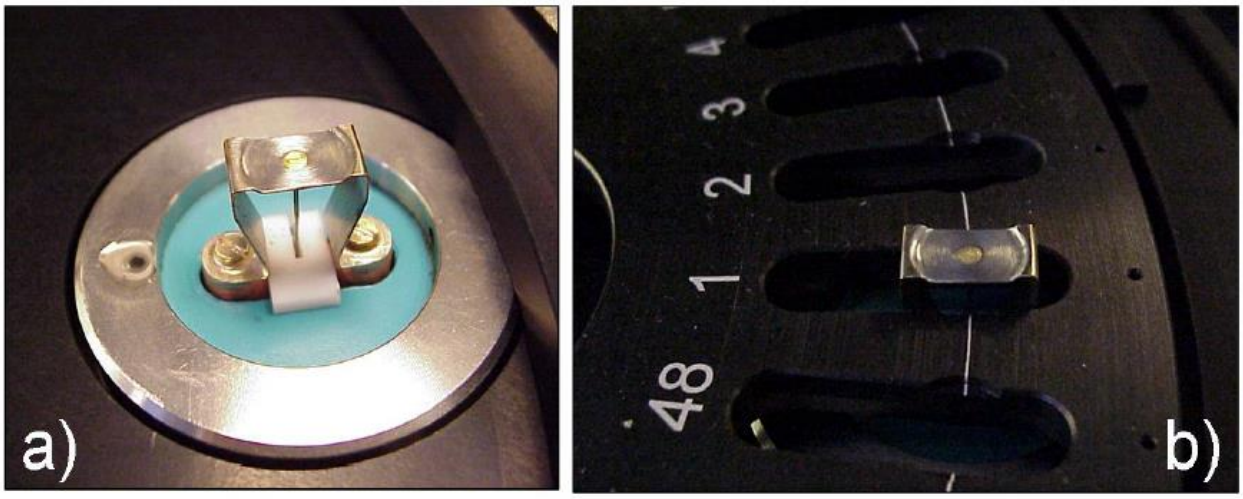

Figure 3.9: a) Picture of the heating element in the measurement position, b) Same as a) but with the sample carrousel in place. The small position holes on the sample carrousel enabling the system to keep track of the position can also be seen.

b) Optical stimulation system

In OSL, the probability of eviction depends on the rate at which photons arrive at the trap and the sensitivity of that particular trap to photo eviction. The sensitivity of the trap depends strongly on the wavelength of the stimulating light, generally the shorter the wavelength the greater the chance of eviction. However, the wavelength of the stimulation light is not the only factor to take into consideration. The wavelength of the emitted luminescence must also be considered. The intensity of the emitted luminescence is many orders of magnitude smaller than the intensity of the stimulation light, so in order to effectively prevent stimulation light from reaching the PMT, the wavelengths of the stimulation light and the luminescence must be well separated or appropriate filters used.

Conventionally, the samples are stimulated at constant light intensity (continuous wave CW-mode), which produces an exponentially decaying signal as the electron traps are being depleted. However, the decay curves for most samples contain more than one component (i.e., traps with different optical cross-sections), and require several exponential functions to adequately describe the data. In linearly modulated

OSL (LM-OSL) the stimulation light intensity is varied linearly (usually from zero to a predefined value).

Electrons in traps most sensitive to light will be evicted at low intensities, whereas the less light sensitive traps will empty at higher intensities. Thus, by ramping the light intensity a stimulation curve is obtained in which different peaks represent different sensitivities to light (Bulur, 1996). In pulsed OSL (POSL, McKeever et al., 1996) the stimulation light is pulsed and the OSL is only measured in between the pulses (see Figure 3.10). Pulsing provides insight into the luminescence recombination process, reduces the need for filtering and provides an instrumental way of separating the luminescence emitted from different phosphors.

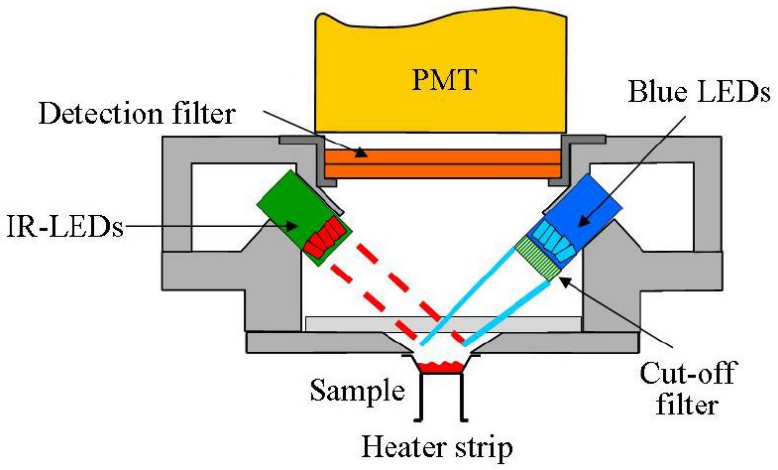

Figure 3.10: Schematic diagram of the combined blue and IR LED OSL unit.

In the standard Riso TL/OSL reader (Botter-Jensen et al., 2000) a choice of two stimulation sources exists: 1) infrared (IR) light emitting diodes (LEDs) and 2) blue LEDs (see Figure 2.9). LEDs are inexpensive, compact, have short response times and the illumination power density can be controlled electronically. The latter offers the possibility of stimulation at different intensities and varying the stimulation intensity as a function of stimulation time. The array of LEDs is equipped with an optical feedback servo-system to ensure the stability of the stimulation power. Stimulation in CW-mode and LM-mode is possible in all Riso readers. Stimulation in pulsed mode requires additional hardware and is only offered as an additional option.

The LEDs are arranged in clusters, which are mounted concentrically in a ring-shaped holder located between the heater element and the photomultiplier tube. The holder is machined so that all individual diodes are focused at the sample. Each cluster contains seven LEDs and the ring-shaped holder can contain up to seven clusters (i.e. a total of 49 LEDs). The distance between the diodes and the sample is approximately 20 mm. A picture of the OSL stimulation unit is shown in Figure 3.11.

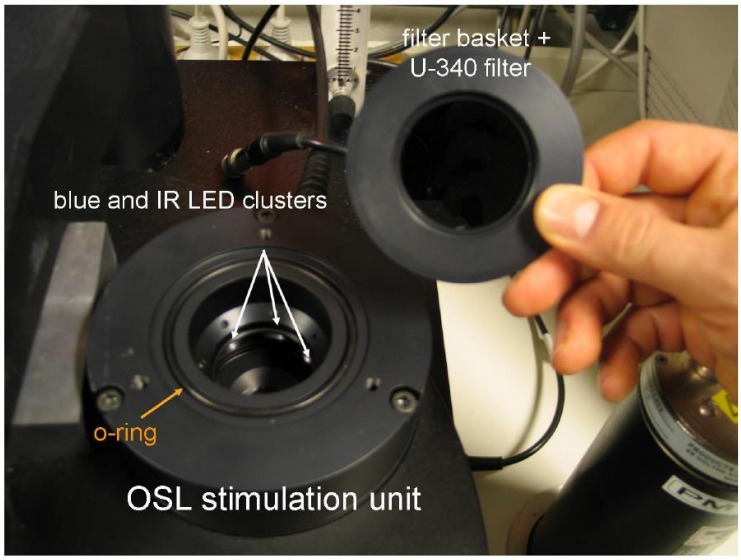

Figure 3.11: Picture of the OSL stimulation unit and the U-340 detection filter.

(c)Blue LEDs

The Riso reader is equipped with blue LEDs (NICHIA type NSPB-500AS) with a peak emission at 470 nm (FWHM = 20 nm). They have an emission angle of 15 degrees and a power output of ~4.8cd at 20 mA. The blue LEDs are usually arranged in 4 clusters each containing seven individual LEDs. The total power from 28 LEDs is 80 mW/cm2 at the sample position (Botter-Jensen et al., 2003). The advantage of using the stimulation spectrum from the blue LEDs is that the OSL decay will be rapid because of the short wavelength, but the disadvantage is that the spectrum has a significant tail into the detection window (centered on 340 nm). To reduce the intensity of this tail, and thereby minimize the amount of directly scattered blue light reaching the light detection system, a green long pass filter (GG-420) is incorporated in front of each blue LED cluster. The filter effectively attenuates the high energy photons from the blue LEDs at the cost of approximately 5% attenuation of the peak centered on 470 nm. Figure 3.12 displays the measured LED emission spectrum compared with the published transmission curve for the GG-420 filter and the U-340 detection filter.

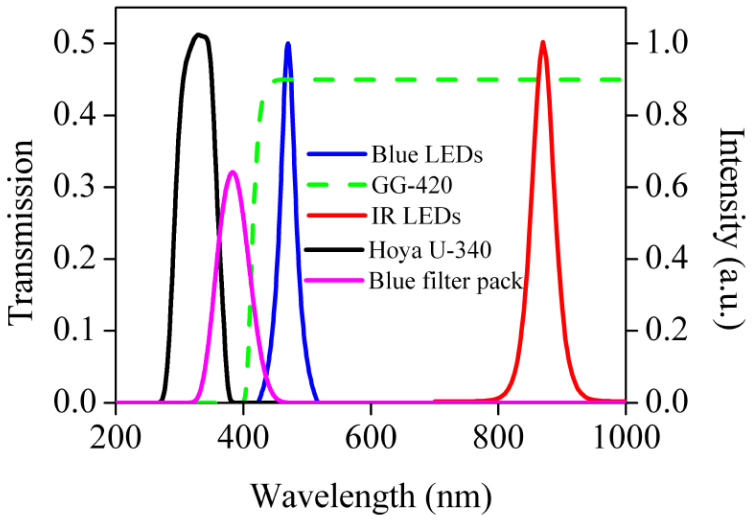

When stimulating with the blue LEDs only the U-340 detection filter can be used. SWITCHING ON THE BLUE LED'S WITH THE BLUE FILTER PACK IN PLACE WILL SERIOUSLY DAMAGE THE PMT.

Figure 3.12: The emission spectrum of IR and blue

3.9 Experimental Protocols used in the present work

1) Effect of beta dose on TL glow curve of unannealed sample.

	SQ (grain size 63-53µm)
Step-1	**Unannealed sample**
Step-2	**Beta Dose**
	2.268 Gy, 22.68 Gy, 158.76 Gy @Dose Rate 4.45 ± 0.06Gy/min
Step-3	**TL record from 0-450°C @heating rate 5°C /sec**

2) Effect of annealing temperature on TL glow curve of sample.

	SQ (grain size 63-53µm)
Step-1	**Annealing; 400^{0}C, 600^{0}C, 800^{0}C, 1000^{0}C @1hr and quenched at RT**
Step-2	**Beta Dose 2.268 Gy, 22.68 Gy, 158.76 Gy @Dose Rate 4.45 ± 0.06Gy/min**
Step-3	**TL records from 0-450^{0}C @heating rate 5 °C /sec**

3) Effect of cyclic physical treatment on TL glow curve of annealed sample.

	SQ(Grain Size 63-53µm)		
Step-1	**Annealing; 400^0C, 600^0C, 800^0C, 1000^0C @1hr and quenched at RT**		
Step-2	**Beta 2.268 Gy (D_0)**	**Do**	
Step-3	**TB-1 from 0^0C -200^0C**	**Sequence**	**TL-1 Record from 0^0C -200^0C**
	TB-2 from 0^0C -450^0C		
	Test Dose (TD)0.756 Gy		
	TB-1 from 0^0C -200^0C		
	TB-2 from 0^0C -450^0C		
Step-4	**Beta 22.68 Gy(D_1)**	**D_1**	
Step-3	**TB-1 from 0^0C -200^0C**	**Sequence**	**TL-2 Record from 0^0C -200^0C**
	TB-2 from 0^0C -450^0C		
	Test Dose (TD)0.756 Gy		
	TB-1 from 0^0C -200^0C		
	TB-2 from 0^0C -450^0C		
Step-5	**Beta 75.6 Gy(D_2)**	**D_2**	
Step-3	**TB-1 from 0^0C -200^0C**	**Sequence**	**TL-3 Record from 0^0C -200^0C**
	TB-2 from 0^0C -450^0C		
	Test Dose (TD)0.756 Gy		
	TB-1 from 0^0C -200^0C		
	TB-2 from 0^0C -450^0C		
Step-6	**Beta 151.2 Gy(D_3)**	**D_3**	
Step-3	**TB-1 from 0^0C -200^0C**	**Sequence**	**TL-4 Record from 0^0C -200^0C**
	TB-2 from 0^0C -450^0C		
	Test Dose (TD)0.756 Gy		
	TB-1 from 0^0C -200^0C		

	TB-2 from 0^0C -450^0C		
Step-2	**Beta 2.268 Gy (Do)**	**Do**	
Step-7	**TB-1 from 0^0C -200^0C**		**TL-5 Record from 0^0C -200^0C**

4) TL from 0^0C -450^0C for annealed sampled at different cyclic sequence of physical condition

	SQ (Grain Size 63-53µm)		
Step-1	**Annealing; 400^0C, 600^0C, 800^0C,1000^0C@1hr and quenched at RT**		
Step-2	**Beta 2.268 Gy (D_0)**	**Do**	
Step-3	**TB-1 from 0^0C -200^0C**	**Sequence**	
	TB-2 from 0^0C -450^0C		**TL-1 Record from 0^0C -450^0C**
	Test Dose (TD)0.756 Gy		
	TB-1 from 0^0C -200^0C		
	TB-2 from 0^0C -450^0C		
Step-4	**Beta 22.68Gy(D_1)**	**D_1**	
Step-3	**TB-1 from 0^0C -200^0C**	**Sequence**	
	TB-2 from 0^0C -450^0C		**TL-2 Record from 0^0C -450^0C**
	Test Dose (TD)0.756 Gy		
	TB-1 from 0^0C -200^0C		
	TB-2 from 0^0C -450^0C		
Step-5	**Beta 75.6Gy(D_2)**	**D_2**	
Step-3	**TB-1 from 0^0C -200^0C**	**Sequence**	
	TB-2 from 0^0C -450^0C		**TL-3 Record from 0^0C -450^0C**
	Test Dose (TD)0.756 Gy		
	TB-1 from 0^0C -200^0C		
	TB-2 from 0^0C -450^0C		
Step-6	**Beta 151.2Gy(D_3)**	**D_3**	
Step-3	**TB-1 from 0^0C -200^0C**	**Sequence**	

	TB-2 from 0^0C -450^0C		**TL-4 Record from 0^0C -450^0C**
	Test Dose (TD)0.756 Gy		
	TB-1 from 0^0C -200^0C		
	TB-2 from 0^0C -450^0C		
Step-2	**Beta 2.268Gy (D_0)**	**Do**	
Step-7	**TB-1 from 0^0C -200^0C**		
Step-8	**TB-2 from 0^0C -450^0C**		**TL-5 Record from 0^0C -450^0C**

5) Effect of repetition of cyclic sequence of physical condition on OSL decay.

	SQ (Grain Size 63-53µm)		
Step-1	**400^0C, 600^0C, 800^0C and 1000^0C Annealed @ 1 hour**		
Step-2	**Beta 2.268Gy (D_0)**	**D_0**	
Step-3	**Thermal Bleaching-1(0^0C -200^0C)**	**Sequence**	
	Optical Bleaching for 40 sec at 125^0C		**Recorded OSL-1 at 125^0C**
	TD 0.756Gy		
	Thermal Bleaching-1(0^0C -200^0C)		
	Optical Bleaching for 40 sec at 125^0C		
Step-4	**Beta 22.68Gy(D_1)**	**D_1**	
Step-3	**Thermal Bleaching-1(0^0C -200^0C)**	**Sequence**	
	Optical Bleaching for 40 sec at 125^0C		**Recorded OSL-2 at 125^0C**
	TD 0.756Gy		
	Thermal Bleaching-1(0^0C -200^0C)		
	Optical Bleaching for 40 sec at 125^0C		
Step-5	**Beta 75.6Gy(D_2)**	**D_2**	
Step-3	**Thermal Bleaching-1(0^0C -200^0C)**	**Sequence**	

	Optical Bleaching for 40 sec at 125^0C		**Recorded OSL-3 at 125^0C**
	TD 0.756Gy		
	Thermal Bleaching-1(0^0C -200^0C)		
	Optical Bleaching for 40 sec at 125^0C		
Step-6	**Beta 151.2Gy(D_3)**	**D_3**	
Step-3	**Thermal Bleaching-1(0^0C -200^0C)**	**Sequence**	
	Optical Bleaching for 40 sec at 125^0C		**Recorded OSL-4 at 125^0C**
	TD 0.756Gy		
	Thermal Bleaching-1(0^0C -200^0C)		
	Optical Bleaching for 40 sec at 125^0C		
Step-2	**Beta 2.268Gy(D_0)**	**D_0**	
Step-6	**Thermal Bleaching-1(0^0C -200^0C)**		
Step-7	**Optical Bleaching for 40 sec at 125^0C**		**Recorded OSL-5 at 125^0C**

6) Deconvolution study of OSL at 125 oC under sequence of physical condition

	SQ (Grain Size 63-53µm)		
Step-1	**400^0C, 600^0C, 800^0C and 1000^0C Annealed @ 1 hour and quenched at RT**		
Step-2	**Beta 2.268Gy (D_0) @ Dose Rate**	**D_0**	
Step-3	**Thermal Bleaching-1(0^0C -200^0C)**	**Sequence**	
	Optical Bleaching for 40 sec at 125^0C		
	TD 0.756Gy		
	Thermal Bleaching-1(0^0C -200^0C)		
	Optical Bleaching for 40 sec at 125^0C		**Recorded OSL-1 at 125^0C**
Step-4	**Beta 22.68Gy(D_1)**	**D_1**	
Step-3	**Thermal Bleaching-1(0^0C -200^0C)**	**Sequence**	
	Optical Bleaching for 40 sec at 125^0C		

	TD 0.756Gy		
	Thermal Bleaching-1(0^0C -200^0C)		
	Optical Bleaching for 40 sec at 125^0C		**Recorded OSL-2 at 125^0C**
Step-5	**Beta 75.6Gy(D_2)**	**D_2**	
Step-3	**Thermal Bleaching-1(0^0C -200^0C)**	**Sequence**	
	Optical Bleaching for 40 sec at 125^0C		
	TD 0.756Gy		
	Thermal Bleaching-1(0^0C -200^0C)		
	Optical Bleaching for 40 sec at 125^0C		**Recorded OSL-3 at 125^0C**
Step-6	**Beta 151.2Gy (D_3)**	**D_3**	
Step-3	**Thermal Bleaching-1(0^0C -200^0C)**	**Sequence**	
	Optical Bleaching for 40 sec at 125^0C		
	TD 0.756Gy		
	Thermal Bleaching-1(0^0C -200^0C)		
	Optical Bleaching for 40 sec at 125^0C		**Recorded OSL-4 at 125^0C**
Step-2	**Beta 2.268Gy(D_0)**	**D_0**	
Step-3	**Thermal Bleaching-1(0^0C -200^0C)**		
	Optical Bleaching for 40 sec at 125^0C		
	TD 0.756Gy		
	Thermal Bleaching-1(0^0C -200^0C)		
	Optical Bleaching for 40 sec at 125^0C		**Recorded OSL-5 at 125^0C**

References:

1. McKeever, S. W. et al. Recent advances in dosimetry using the optically stimulated luminescence of Al2O3: C. Radiation protection dosimetry109, 269-276 (2004).
2. Chruścińska, A. On some fundamental features of optically stimulated luminescence measurements. Radiation Measurements45, 991-999 (2010)
3. Yadav, L. in Organic Spectroscopy 224-249 (Springer, 2005).
4.https://www.nutech.dtu.dk/english/Products-and-Services/Radiation-Instruments/
5. P Saha, Annamalai and A.fLGuha, " Synthetic Quartz production and Applications", Transaction ofIndian Ceramic Society, vol-50 (5), Sept-Oct, 1991.